

## Higher-Twist Dynamics in Large Transverse Momentum Hadron Production

François Arleo,<sup>1</sup> Stanley J. Brodsky,<sup>2,3</sup> Dae Sung Hwang,<sup>4</sup> and Anne M. Sickles<sup>5</sup>

<sup>1</sup>LAPTH, UMR5108, Université de Savoie, CNRS, BP 110, 74941 Annecy-le-Vieux cedex, France

<sup>2</sup>SLAC National Accelerator Laboratory, Stanford University, Stanford, California 94309, USA

<sup>3</sup>CP3-Origins Southern Denmark University Odense, Denmark

<sup>4</sup>Department of Physics, Sejong University, Seoul 143-747, Korea

<sup>5</sup>Brookhaven National Laboratory, Upton, New York 11973, USA

(Received 27 November 2009; published 6 August 2010)

A scaling law analysis of the world data on inclusive large- $p_{\perp}$  hadron production in hadronic collisions is carried out. Significant deviations from leading-twist perturbative QCD predictions at next-to-leading order are observed, particularly at high  $x_{\perp} = 2p_{\perp}/\sqrt{s}$ . In contrast, the production of prompt photons and jets exhibits near-conformal scaling behavior in agreement with leading-twist expectations. These results indicate a non-negligible contribution of higher-twist processes in large- $p_{\perp}$  hadron production, where the hadron is produced directly in the hard subprocess, rather than by quark and gluon fragmentation. Predictions for the scaling exponents at RHIC and LHC are given. Triggering on isolated large- $p_{\perp}$  hadron production will enhance the higher-twist processes. We also note that the use of isolated hadrons as a signal for new physics can be affected by the presence of direct hadron production.

DOI: 10.1103/PhysRevLett.105.062002

PACS numbers: 12.38.Bx, 12.38.Qk, 13.85.Ni

The production of a hadron at large transverse momentum,  $p_{\perp}$ , in a hadronic collision is conventionally analyzed within the framework of perturbative QCD (pQCD) by convoluting the leading-twist (LT)  $2 \rightarrow 2$  hard subprocess cross sections with evolved parton distribution functions (PDFs) and fragmentation functions (FFs). The most important discriminant of the twist of a pQCD subprocess in a hard hadronic collision is the scaling of the inclusive invariant cross section [1]

$$\sigma^{\text{inv}} \equiv E \frac{d\sigma}{d^3p} (AB \rightarrow CX) = \frac{F(x_{\perp}, \vartheta)}{p_{\perp}^n}, \quad (1)$$

at fixed  $x_{\perp} = 2p_{\perp}/\sqrt{s}$  and center-of-mass (c.m.) angle  $\vartheta$ . In the original parton model the power falloff is simply  $n = 4$  since the underlying  $2 \rightarrow 2$  subprocess amplitude for pointlike partons is scale invariant, and there is no dimensionful parameter as in a conformal theory. However, in general additional higher-twist (HT) contributions involving a larger number of elementary fields contributing to the hard subprocess,  $n_{\text{active}} > 4$ , are also expected. For example, the detected hadron  $C$  can be produced directly in the hard subprocess reaction as in an exclusive reaction. Such direct HT processes can give a significant contribution since there is no suppression from jet fragmentation at large momentum fraction carried by the hadron,  $z$ , and the trigger hadron is produced without any waste of energy.

Apart from the scaling violations in QCD, the invariant cross section of a given hard subprocess is expected to scale quite generally as (neglecting spin corrections) [2]

$$\sigma^{\text{inv}}(AB \rightarrow CX) \propto \frac{(1 - x_{\perp})^{2n_{\text{spectator}} - 1}}{p_{\perp}^{2n_{\text{active}} - 4}}, \quad (2)$$

where  $n_{\text{spectator}}$  is the number of constituents of  $A$ ,  $B$ , and  $C$  not participating in the subprocess. From Eq. (2), HT

processes involving a large number of active fields will result in a  $p_{\perp}$  exponent larger than the LT expectation ( $n > 4$ ), but will exhibit a slower falloff with  $x_{\perp}$  from the smaller number of spectator fields. Therefore, at large  $x_{\perp}$  and not too large  $p_{\perp}$ , HT contributions to the cross section can become significant. In Ref. [3] the cross sections of the HT subprocesses  $gq \rightarrow \pi q$  and  $q\bar{q} \rightarrow \pi g$ , where the pion (twist 2) is produced directly, have been calculated quantitatively in pQCD, leading to a contribution to  $\sigma^{\text{inv}}$  with nominal scaling  $n = 6$  since  $n_{\text{active}} = 5$  [3]. In the case of baryon (twist 3) direct production,  $n_{\text{active}} = 6$  leading to nominal scaling  $n = 8$  [1]. In the case of photons and jets, the number of active fields is  $n_{\text{active}} = 4$  leading to scaling exponents  $n = 4$  in the conformal limit.

The idea of direct hadron production was considered in the 1970s to explain the large fixed- $x_{\perp}$  scaling exponents reported at ISR and fixed target Fermilab energies [1]. However, there has been no comprehensive and quantitative analysis of the data up to now which could bring compelling evidence for such HT effects. In this Letter, we revisit the possible presence of HT effects in large- $p_{\perp}$  hadron production. The three novel aspects of this analysis are (i) a dedicated analysis of the most recent Fermilab, RHIC and Tevatron data on large- $p_{\perp}$  hadrons, prompt photons and jets, (ii) the systematic comparison of the experimental scaling exponents with next-to-leading order (NLO) QCD expectations, and (iii) predictions for the top RHIC energy and the LHC. The results have strong impact on the interpretation of high  $p_{\perp}$  hadroproduction in QCD. They are also crucial for understanding the baryon anomaly in heavy-ion collisions at RHIC.

The exponent  $n^{\text{NLO}}$  of midrapidity particle production ( $\vartheta = \pi/2$ ) is computed in QCD at NLO accuracy from

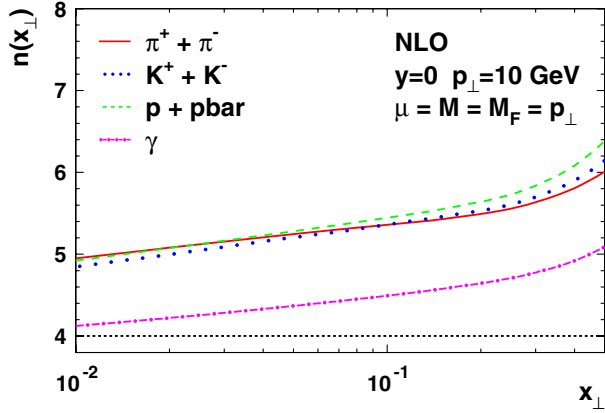


FIG. 1 (color online).  $x_{\perp}$  dependence of  $n^{\text{NLO}}$  for  $\pi^{\pm}$  (solid line),  $K^{\pm}$  (dotted line),  $p/\bar{p}$  (dashed line) and  $\gamma$  (dot-dashed line), at  $p_{\perp} = 10$  GeV.

[4], with CTEQ6.6 [5] PDFs and the de Florian-Sassot-Stratmann and Bourhis-Fontannaz-Guillet FFs into hadrons and photons [6], respectively. The  $x_{\perp}$ -dependence of  $n^{\text{NLO}}$  at fixed  $p_{\perp} = 10$  GeV is shown in Fig. 1 for pions, kaons, protons plus antiprotons, and inclusive prompt photons. The hadron exponents increase slowly from  $n^{\text{NLO}} \simeq 5$  at small values of  $x_{\perp}$  ( $x_{\perp} = 10^{-2}$ ) up to  $n^{\text{NLO}} \simeq 6$  at  $x_{\perp} = 0.5$  with very little dependence on the specific hadron species. The exponent extracted in the prompt photon channel is below those of hadrons, by roughly one unit. The smaller photon exponent is understood from the (relative) absence of fragmentation processes and one less power in  $\alpha_s$ , leading to less scaling violation in this channel. Remarkably,  $n_{\gamma}^{\text{NLO}}$  is close to the conformal limit,  $n = 4$ , at the smallest values of  $x_{\perp}$ .

In order to investigate possible HT dynamics in large- $p_{\perp}$  hadron production,  $n^{\text{exp}}$  has been systematically extracted from measurements in  $p$ - $p$  and  $p$ - $\bar{p}$  collisions, from fixed-target to collider experiments, and compared to LT QCD expectations. It is deduced from the comparison of  $x_{\perp}$  spectra at different c.m. energies,

$$n^{\text{exp}}(x_{\perp}) \equiv - \frac{\ln(\sigma^{\text{inv}}(x_{\perp}, \sqrt{s_1})/\sigma^{\text{inv}}(x_{\perp}, \sqrt{s_2}))}{\ln(\sqrt{s_1}/\sqrt{s_2})} \quad (3)$$

TABLE I. Data sets selected in the present Letter. The kinematical range ( $\sqrt{s}$ ,  $p_{\perp}$  in GeV), the mean  $\langle n^{\text{exp}} \rangle$  extracted from each set composed of  $n_{\text{data}}$  data points and the corresponding expectation in QCD at NLO,  $\langle n^{\text{NLO}} \rangle$ , are given.

Exp.	Ref.	Species	$\sqrt{s}$	$p_{\perp}$	$x_{\perp}$	$n_{\text{data}}$	$\langle n^{\text{exp}} \rangle$	$\langle n^{\text{NLO}} \rangle$
E706	[9]	$\pi^0$	31.6, 38.8	2 – 9	$10^{-1} - 4 \times 10^{-1}$	25	$8.2 \pm 0.11$	$6.1 \pm 0.09$
PHENIX/ISR	[7,8]	$\pi^0$	62.4, 22.4	2 – 7	$2 \times 10^{-1} - 2 \times 10^{-1}$	3	$7.5 \pm 0.19$	$6.2 \pm 0.30$
PHENIX	[7,10]	$\pi^0$	62.4, 200	2 – 19	$7 \times 10^{-2} - 2 \times 10^{-1}$	12	$6.7 \pm 0.05$	$5.6 \pm 0.08$
UA1	[11]	$h^{\pm}$	500, 900	2 – 9	$8 \times 10^{-3} - 2 \times 10^{-2}$	18	$5.7 \pm 0.09$	$5.2 \pm 0.04$
CDF	[12]	$h^{\pm}$	630, 1800	2 – 9	$7 \times 10^{-3} - 10^{-2}$	5	$5.2 \pm 0.15$	$5.0 \pm 0.07$
CDF	[13]	tracks	630, 1800	2 – 19	$7 \times 10^{-3} - 2 \times 10^{-2}$	52	$5.7 \pm 0.03$	$5.0 \pm 0.02$
CDF	[14]	$\gamma$	630, 1800	11 – 81	$3 \times 10^{-2} - 9 \times 10^{-2}$	7	$4.7 \pm 0.09$	$4.3 \pm 0.01$
D0	[15,16]	$\gamma$	630, 1800	11 – 107	$3 \times 10^{-2} - 10^{-1}$	6	$4.5 \pm 0.12$	$4.3 \pm 0.01$
CDF	[17]	jets	546, 1800	29 – 190	$10^{-1} - 2 \times 10^{-1}$	9	$4.3 \pm 0.09$	$4.6 \pm 0.01$
D0	[18]	jets	630, 1800	23 – 376	$8 \times 10^{-2} - 4 \times 10^{-1}$	23	$4.5 \pm 0.04$	$4.6 \pm 0.01$

which is equivalent to (1) at fixed  $x_{\perp}$ . In order to reduce systematic uncertainties, only experiments which measured  $x_{\perp}$  spectra at two distinct c.m. energies are considered, except for the PHENIX results at  $\sqrt{s} = 62.4$  GeV [7] compared to a fit of ISR measurements at  $\sqrt{s} = 22.4$  GeV [8]. The recent data analyzed in this Letter are summarized in Table I. The data sets include  $\pi^0$  measurements by the E706 at Fermilab [9] and by the PHENIX collaboration at RHIC [7,10]. At higher energies, the measurements of charged hadrons (or charged tracks [13]) in  $p$ - $\bar{p}$  collisions at  $\sqrt{s} = 630, 1800$  GeV by CDF [12,13] and  $\sqrt{s} = 500, 900$  GeV by UA1 [11] are included in the analysis. Also considered are prompt photon [14–16] and jet [17,18] data obtained by CDF and D0 at  $\sqrt{s} = 546, 630, 1800$  GeV.

The hadron exponents plotted in Fig. 2 (left) exhibit a clear trend, with a significant rise of  $n^{\text{exp}}$  as a function of  $x_{\perp}$ . Typical values of  $n^{\text{exp}}$  are  $n^{\text{exp}} \simeq 5$ – $6$  at small  $x_{\perp} \simeq 10^{-2}$  while PHENIX data point to a mean value  $n^{\text{exp}} \simeq 6.7$  at  $x_{\perp} \simeq 10^{-1}$ . At higher values of  $x_{\perp}$ , the comparison of PHENIX with ISR data as well as the E706 measurements reveal an exponent even larger:  $n^{\text{exp}} \simeq 7.5$  ( $x_{\perp} = 0.2$ ) and  $n^{\text{exp}} \simeq 8.2$  ( $x_{\perp} = 0.2$ – $0.4$ ), respectively. The E706 data clearly confirm results reported long ago at the ISR [1]. The results obtained in the photon and jet channels are strikingly different from what is observed for hadrons. Their exponents show little dependence on  $x_{\perp}$ , yet the data cover a wide complementary range. Importantly, the values obtained lie only slightly above the conformal limit,  $n_{\gamma}^{\text{exp}} \simeq 4.6$  and  $n_{\text{jets}}^{\text{exp}} \simeq 4.4$ ; most significantly they are several units smaller than the hadron exponents taken at the same  $x_{\perp}$  (the  $p_{\perp}$  range being however different).

In order to compare properly data and theory, NLO calculations have also been carried out within the same kinematical conditions as the experiments. The difference between experimental and theoretical exponents,  $\Delta(x_{\perp}) \equiv n^{\text{exp}} - n^{\text{NLO}}$ , is plotted in the right panel of Fig. 2 for hadrons, photons, and jets. Note that the error bars include both experimental *as well as* theoretical errors, added in quadrature. The biggest theoretical uncertainty comes from the variation of renormalization and factorization scales from  $p_{\perp}/2$  to  $2p_{\perp}$ . Figure 2 (right) indicates that

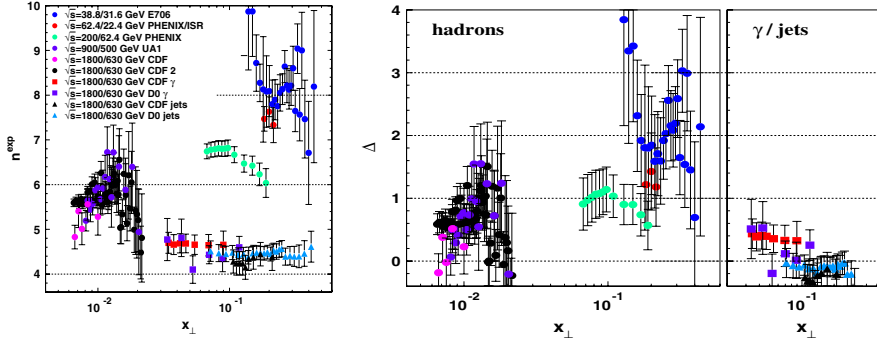


FIG. 2 (color online). Left: Values of  $n^{\text{exp}}$  as a function of  $x_{\perp}$  for  $h^{\pm}/\pi^0$  (circles),  $\gamma$  (squares) and jets (triangles). Right:  $\Delta \equiv n^{\text{exp}} - n^{\text{NLO}}$  as a function of  $x_{\perp}$ , error bars include the experimental and the theoretical uncertainties added in quadrature (see text).

the hadronic exponents extracted experimentally prove to be significantly above the LT predictions. The discrepancy is moderate at small  $x_{\perp}$ ,  $\Delta(x_{\perp} \sim 10^{-2}) \approx 0.5$  (with  $\chi^2/\text{ndf} \equiv 1/N \times \sum_i \Delta_i^2 / \delta \Delta_i^2 = 4.8$ ), but becomes increasingly larger at higher values of  $x_{\perp}$ : the PHENIX measurements at  $x_{\perp} \approx 10^{-1}$  lead to  $\Delta \approx 1$  ( $\chi^2/\text{ndf} = 7.0$ ) and the exponent inferred from E706 data is two units above LT expectations ( $\chi^2/\text{ndf} = 8.0$ ). In contrast, the scaling behaviors observed for photons and jets remarkably coincide, in very good agreement with the NLO predictions (with much smaller  $\chi^2$  values,  $\chi^2/\text{ndf} = 1.8$  and  $\chi^2/\text{ndf} = 2.2$ , respectively). Part of the discrepancy between data and fixed-order calculations at large  $x_{\perp} \sim 1$  could occur because of the appearance of large threshold logarithms,  $\ln(1 - x_{\perp})$ , which should be resummed to all orders [19]. However, the discrepancy is also observed at small values of  $x_{\perp} \sim 10^{-2}$ , where threshold effects are expected to be small.

The most natural explanation for the hadron data is the presence of important HT contributions from processes in which the detected hadron appears in the hard subprocess. The dimension of the hadron distribution amplitude leads naturally to larger exponents. In contrast, particles having no hadronic structure like isolated photons and jets are much less sensitive to such HT contributions and should behave closer to LT expectations, as observed. Also of note are the larger exponents for protons than for pions observed at the ISR. As already mentioned, the exponent of HT would be  $n_{\pi} = 6$  for pions and  $n_p = 8$  for protons, leading to  $n_p - n_{\pi} = 2$  instead of  $n_p - n_{\pi} \approx 0$  at LT (see Fig. 1). The experimental value which we obtain from the ISR,  $n_p - n_{\pi} \approx 1$ , thus reflects the mixture of LT and HT contributions to the total cross section. It has also been noted [20] that the presence of color-transparent HT subprocesses such as  $uu \rightarrow p\bar{d}$  can account for the anomalous features of proton production seen in heavy-ion collisions at RHIC [21].

In order to probe HT contributions more explicitly, let us consider a 2-component model cross section with nominal power dependence

$$\sigma^{\text{model}}(pp \rightarrow \pi X) \propto \frac{A(x_{\perp})}{p_{\perp}^4} + \frac{B(x_{\perp})}{p_{\perp}^6}, \quad (4)$$

corresponding to the LT ( $n_{\text{active}} = 4$ ) and HT ( $n_{\text{active}} = 5$ )

processes, respectively. The actual  $p_{\perp}$  exponents are modified by the running coupling and PDF and FF evolution. Assuming that the contributions to  $n^{\text{NLO}} - 4$  due to pQCD are the same for the LT and HT processes, Eq. (4) gives the *effective* exponent

$$\begin{aligned} n_{\text{eff}}(x_{\perp}, p_{\perp}, B/A) &\equiv -\frac{\partial \ln \sigma^{\text{model}}}{\partial \ln p_{\perp}} + n^{\text{NLO}}(x_{\perp}, p_{\perp}) - 4 \\ &= \frac{2B/A}{p_{\perp}^2 + B/A} + n^{\text{NLO}}(x_{\perp}, p_{\perp}). \end{aligned} \quad (5)$$

As shown in Fig. 3 (solid line), the LT pion exponent (evaluated at  $x_{\perp} = 0.2$ ) slowly decreases with  $p_{\perp}$  and reaches  $n_{\text{eff}} = 4$  as  $p_{\perp} \rightarrow \infty$  because of asymptotic freedom. Equation (5) shows that  $n_{\text{eff}}$  depends on the relative strength of HT corrections to the LT cross section,  $B/A$ . The value  $B/A \sim 50 \text{ GeV}^2$  ( $\chi^2/\text{ndf} = 0.1$ , as compared to  $\chi^2/\text{ndf} = 5.2$  when  $B/A = 0$ ) is extracted from the data as shown in Fig. 3. A somewhat smaller estimate,  $B/A \sim 15 \text{ GeV}^2$ , is obtained when all scales are set to  $p_{\perp}/2$  in the QCD calculation. We note that the HT rate for direct processes and therefore  $B/A$  are enhanced relative to fragmentation processes since the trigger hadron is produced without any waste of energy; thus the magnitude of the subprocess amplitude is maximized since it is evaluated at the trigger  $p_{\perp}$ , and the initial momentum fractions  $x_1$  and  $x_2$  are evaluated at small values where the PDFs are largest.

Finally, we discuss the phenomenological consequences of possible HT contributions to hadron production in  $p$ - $p$  collisions at RHIC and LHC. In order to obtain qualitative predictions, the variable  $\Delta$  has been fitted to the hadron data in Table I using a simple parametrization (with  $\langle p_{\perp} \rangle$  the geometrical mean of the two  $p_{\perp}$  bins)

$$\Delta^{\text{fit}}(x_{\perp}, \langle p_{\perp} \rangle) = p_0 (-\log x_{\perp})^{p_1} \frac{2p_2(1 - x_{\perp})^{p_3}}{\langle p_{\perp} \rangle^2 + p_2(1 - x_{\perp})^{p_3}},$$

inspired by the 2-component model described above. As expected in QCD,  $\Delta^{\text{fit}}$  is vanishing in  $p_{\perp} \rightarrow \infty$  limit at fixed  $x_{\perp}$ . This analytic form is somewhat arbitrary but flexible enough for making predictions beyond the  $(x_{\perp}, p_{\perp})$ -range probed in present experiments. The typical values of  $\Delta^{\text{fit}}$  expected at RHIC (taking  $\sqrt{s} = 200, 500 \text{ GeV}$ ) and at LHC ( $\sqrt{s} = 7 \text{ TeV}$ , compared to  $\sqrt{s} = 1.8 \text{ TeV}$  at Tevatron) are plotted as a function of  $x_{\perp}$  in

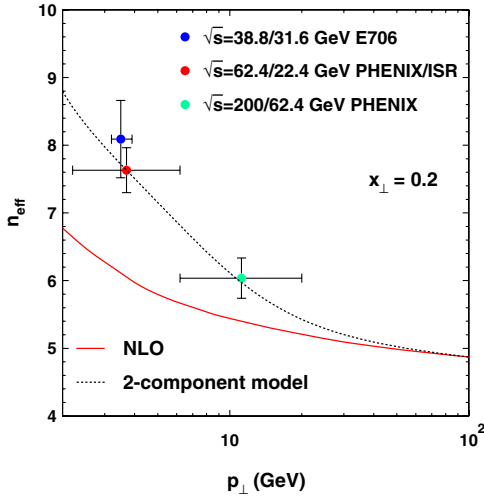


FIG. 3 (color online).  $p_{\perp}$  dependence of  $n_{\text{eff}}$  of pions at  $x_{\perp} = 0.2$  in QCD at NLO (solid line). The dotted line represents a fit based on a two-component model with  $B/A = 50 \text{ GeV}^2$ , see Eq. (5).

Fig. 4. At RHIC,  $\Delta^{\text{fit}}$  is slightly below 1 at small  $x_{\perp} \lesssim 5 \times 10^{-2}$  but decreases towards zero at larger  $x_{\perp}$  (i.e., larger  $p_{\perp}$ ). At LHC, smaller deviations with NLO expectations are expected because of the large values of  $\langle p_{\perp} \rangle$  probed at high energy:  $\Delta^{\text{fit}} \simeq 0.5$  below  $x_{\perp} = 5 \times 10^{-3}$  and smaller above. From this, the ratios of  $x_{\perp}$  spectra can be determined straightforwardly,  $R_{\sqrt{s_1}/\sqrt{s_2}} = (\sqrt{s_2}/\sqrt{s_1})^{\Delta^{\text{fit}} + n^{\text{NLO}}}$ , with  $n^{\text{NLO}} \simeq 5.3$  at RHIC and  $n^{\text{NLO}} \simeq 4.8$  at LHC. In order to enhance the HT contribution to hadron production, we suggest to trigger on *isolated* hadrons, i.e., with small hadronic background in their vicinity. The use of isolation cuts, usually applied for prompt photons, will strongly suppress LT processes. Consequently, the scaling exponents of isolated hadrons are expected to be somewhat larger than those in the inclusive channel. The use of isolated hadrons as a signal for Higgs boson production and other new physics scenarios [22] might

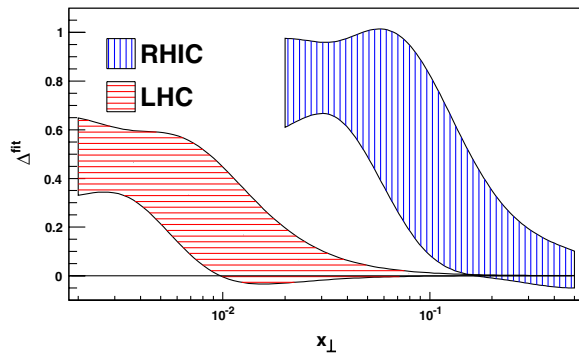


FIG. 4 (color online). Predicted difference between the experimental and NLO scaling exponent at RHIC  $\sqrt{s} = 200, 500 \text{ GeV}$  and the LHC ( $\sqrt{s} = 7 \text{ TeV}$  as compared to  $\sqrt{s} = 1.8 \text{ TeV}$ ) based on a global fit of the hadron production data in Table I.

therefore be confused by the presence of the direct hadron production presently discussed.

The evidence for HT dynamics reported here supports the interpretation of heavy-ion collision measurements at RHIC, in which the dense QCD medium enhances HT contributions, and thus proton production, by filtering LT processes due to partonic energy loss [20]. Future RHIC and LHC measurements will provide further tests of the dynamics of large- $p_{\perp}$  hadron production beyond leading twist.

F. A. thanks P. Aurenche for useful discussions and CERN-TH for hospitality. S.J.B. was supported by the Department of Energy under Contract No. DE-AC02-76SF00515. D.S.H. was supported by the International Cooperation Program of the KICOS and the Korea Research Foundation Grant (KRF-2008-313-C00166). A. M. S. was supported by the Department of Energy under Contract No. DE-AC02-98CH10886.

- [1] S.J. Brodsky and G.R. Farrar, *Phys. Rev. Lett.* **31**, 1153 (1973); D.W. Sivers, S.J. Brodsky, and R. Blankenbecler, *Phys. Rep.* **23**, 1 (1976); R. Blankenbecler, S.J. Brodsky, and J.F. Gunion, *Phys. Rev. D* **18**, 900 (1978); M.J. Tannenbaum, *Proc. Sci.*, (2009) 004 [arXiv:0904.4363].
- [2] S.J. Brodsky, M. Burkardt, and I. Schmidt, *Nucl. Phys. B* **441**, 197 (1995).
- [3] E.L. Berger, T. Gottschalk, and D.W. Sivers, *Phys. Rev. D* **23**, 99 (1981).
- [4] P. Aurenche *et al.*, *Eur. Phys. J. C* **9**, 107 (1999); **13**, 347 (2000); Z. Kunszt and D.E. Soper, *Phys. Rev. D* **46**, 192 (1992).
- [5] J. Pumplin *et al.*, *J. High Energy Phys.* **07** (2002) 012.
- [6] D. de Florian, R. Sassot, and M. Stratmann, *Phys. Rev. D* **75**, 114010 (2007); L. Bourhis, M. Fontannaz, and J.-P. Guillet, *Eur. Phys. J. C* **2**, 529 (1998).
- [7] A. Adare *et al.*, *Phys. Rev. D* **79**, 012003 (2009).
- [8] F. Arleo and D. d'Enterria, *Phys. Rev. D* **78**, 094004 (2008).
- [9] L. Apanasevich *et al.*, *Phys. Rev. D* **68**, 052001 (2003).
- [10] A. Adare *et al.*, *Phys. Rev. D* **76**, 051106 (2007).
- [11] C. Albajar *et al.*, *Nucl. Phys. B* **335**, 261 (1990).
- [12] F. Abe *et al.*, *Phys. Rev. Lett.* **61**, 1819 (1988).
- [13] D.E. Acosta *et al.*, *Phys. Rev. D* **65**, 072005 (2002).
- [14] D.E. Acosta *et al.*, *Phys. Rev. D* **65**, 112003 (2002).
- [15] B. Abbott *et al.*, *Phys. Rev. Lett.* **84**, 2786 (2000).
- [16] V.M. Abazov *et al.*, *Phys. Rev. Lett.* **87**, 251805 (2001).
- [17] F. Abe *et al.*, *Phys. Rev. Lett.* **70**, 1376 (1993).
- [18] B. Abbott *et al.*, *Phys. Rev. D* **64**, 032003 (2001).
- [19] E. Laenen, G. Sterman, and W. Vogelsang, *Phys. Rev. D* **63**, 114018 (2001); N. Kidonakis and J.F. Owens, *Phys. Rev. D* **63**, 054019 (2001); D. de Florian and W. Vogelsang, *Phys. Rev. D* **71**, 114004 (2005).
- [20] S.J. Brodsky and A. Sickles, *Phys. Lett. B* **668**, 111 (2008); S.J. Brodsky, H.J. Pirner, and J. Raufeisen, *Phys. Lett. B* **637**, 58 (2006).
- [21] B.I. Abelev *et al.*, *Phys. Lett. B* **655**, 104 (2007); S.S. Adler *et al.*, *Phys. Rev. Lett.* **91**, 172301 (2003).
- [22] A. Nisati and Y. Sirois (private communication).